

# Sub-Micron Full-Color LED Pixels for Micro-Displays and Micro-LED Main Displays

Xianhe Liu<sup>&,\*</sup>, Yuanpeng Wu<sup>&</sup>, Yakshita Malhotra<sup>&</sup>, Yi Sun<sup>&</sup>, Yong-Ho Ra<sup>\*</sup>, Renjie Wang<sup>\*</sup>,  
Matthew Stevenson<sup>\*\*</sup>, Seth Coe-Sullivan<sup>\*\*</sup> and Zetian Mi<sup>\*,&</sup>

<sup>\*</sup>McGill University Montreal, Canada

<sup>\*\*</sup>NS Nanotech, Ann Arbor, MI, [seth@nsnanotech.com](mailto:seth@nsnanotech.com)

<sup>&</sup>University of Michigan, Ann Arbor

## Abstract

We demonstrate a bottom-up approach to the construction of micro-LEDs as small as 150nm in lateral dimension. Molecular Beam Epitaxy (MBE) is used to fabricate such nanostructured LEDs from InGa<sub>N</sub>, from the blue to red regions of the spectrum, providing a single material set useful for an entire RGB display.

## Author Keywords

Nanowire; quantum dot; GaN; light emitting diode; display; selective area growth.

## 1. Introduction

Selective area molecular beam epitaxy (MBE) is used to fabricate disc-in-nanowire light emitting devices.<sup>1</sup> The optical and electrical properties of InGa<sub>N</sub>/Ga<sub>N</sub> quantum discs depend critically on nanostructure diameter. Photoluminescence (PL) emission of single InGa<sub>N</sub>/Ga<sub>N</sub> nanostructures exhibit a consistent redshift with decreasing diameter. This is due to the increased indium (In) incorporation for nanostructures with small diameters, because of the enhanced contribution of In incorporation from lateral diffusion of In adatoms during growth. Single InGa<sub>N</sub>/Ga<sub>N</sub> nano-LEDs with peak emission wavelengths tuned through nearly the entire visible spectrum on a single chip are demonstrated by varying solely the diameter of the nanostructures. Such nano-LEDs also exhibit superior electrical characteristics, with low turn-on voltage and negligible leakage current. The integration of full-color nano-LEDs on a single chip, coupled to tunable spectral characteristics at the single nanowire level, provides a new and unique approach for realizing efficient micro-LED displays, microdisplays, and backlighting.

## 2. Background

Submicron scale, high efficiency, multi-color light sources monolithically integrated on a single chip are required by the display technologies of tomorrow.<sup>2</sup> Ga<sub>N</sub>-based LEDs are bright, stable and efficient, but are produced in one color across an entire wafer.<sup>3</sup> Achieving efficient green and red LEDs using Ga<sub>N</sub>-based technology has also proven stubbornly difficult. To this date, there is no proven technology to vary In compositions in quantum wells across a wafer to achieve multi-color emission on one substrate.<sup>4,5</sup> InGa<sub>N</sub> nanowire structure studies have shown promise to solve such critical challenges. Nanostructured LEDs exhibit low dislocation densities and improved light extraction efficiency.<sup>6</sup> Multi-colored emission can be demonstrated from InGa<sub>N</sub> nanowire arrays integrated on a single chip.<sup>7,8</sup> Thus, display technologies based on nano-LED pixel arrays integrated on a single chip could become the ultimate emissive light source for three dimensional (3D) projection displays, flexible displays, and even virtual retinal display (VRD) technologies.<sup>9-12</sup> The emission cone and direction can be tailored by the one-dimensional columnar design of each nanostructure,<sup>13</sup> essential to realizing ultrahigh definition

displays. In addition, pixel arrays of single nano-LEDs can increase heat dissipation and can operate at extremely high current densities.<sup>14</sup> Critical to these emerging technology areas is the realization of full-color, tunable emitters including LEDs and lasers, on a single chip. This requires fine tuning of alloy composition in different nano-structured regions, and that these compositional variations are made in a single process step. Sekiguchi et al. reported that such an approach was possible.<sup>15</sup> This method took advantage of a shadow effect of nearest-neighbor structures to vary InGa<sub>N</sub> composition. To date, however, there is no known mechanism to controllably vary alloy compositions structure by structure without modifying global growth parameters. The single-step fabrication of multi-color, nano-LEDs on the same chip has thus not been realized previously.

Hence the significance of this demonstration of single nanowire multi-color LEDs monolithically integrated on a single substrate, which is achieved by incorporating multiple InGa<sub>N</sub>/Ga<sub>N</sub> quantum discs in Ga<sub>N</sub> nanowires of various diameters grown in selective area epitaxy in a single MBE process step. In previous work it is shown that for small diameter nanowires, high In content quantum discs are formed.<sup>1</sup> With increasing nanowire diameter, however, In content is reduced in the critical emissive regions of the device. By exploiting such unique diameter-dependent emission region formation, tunable emission across wide spectral ranges can be achieved in a single MBE process step. Red, orange, green, and blue InGa<sub>N</sub>/Ga<sub>N</sub> nanowire LEDs are formed simultaneously on the same chip, with representative current-voltage curves and strong visible light emission. This offers a new avenue for achieving multi-primary optoelectronic devices at the nanometer level on a single chip for many applications, including imaging, displays, sensing, spectroscopy, and communications. The potential impact in micro-LEDs and microdisplays is clear.

## 3. Results – PL and EL

### Tunable Photoluminescent Nanostructures

Single InGa<sub>N</sub> nanostructures of various diameters have been fabricated on a single substrate by selective area growth (SAG) using radio frequency plasma-assisted MBE. An n-type Ga<sub>N</sub> template on sapphire substrate is used, with a thin (10 nm) Ti layer as a growth mask.<sup>16, 17</sup> 80 nm to 1.9 μm openings were created on the Ti mask. These openings lead to precise control of the nanostructure diameter, which in turn controls nano-LED emission spectrum. As depicted in Figure 1a, each nanowire contains ~ 0.35 μm Ga<sub>N</sub>, five vertically aligned InGa<sub>N</sub>/Ga<sub>N</sub> quantum discs and a 0.5 μm Ga<sub>N</sub> capping layer. A Veeco GENxplor MBE system was used to grow these structures. The Ga<sub>N</sub> is grown with a 1030 °C substrate temperature which is subsequently reduced for active region growth. An optimum temperature of 810 °C was identified for the active region

This is the author manuscript accepted for publication and has undergone full peer review but has not been through the copyediting, typesetting, pagination and proofreading process, which may lead to differences between this version and the Version of Record. Please cite this article as doi: 10.1002/smi.899

growth. Here the temperature refers to the thermocouple reading, which may be different from the substrate surface temperature. Scanning electron microscopy (SEM) images of the single nano-structures grown with various diameters are shown in Figure 1b. The structures exhibit near-perfect hexagonal shape and based on the terminating facets possess Ga-polarity.<sup>18</sup> Photoluminescence (PL) emission for single structures was measured at room-temperature with a 405 nm laser as the excitation source. Figure 1c shows how peak emission wavelength varies with diameter. PL structures were grown in a single MBE process step, and the color tuning is due to the variation of structure diameter within the range of 150 nm to 2  $\mu\text{m}$ . The PL emission shows a consistent blueshift as diameter increases, the opposite effect than that observed when quantum confinement dominates. For example, the emission wavelengths can be tuned from 640 nm to 465 nm as diameters are controlled from 150 nm to 2  $\mu\text{m}$ , all while keeping growth conditions constant. Such trends of diameter vs center wavelength can be modified by changing the growth temperature and keeping the diameter range constant. PL emission spectra of different diameter structures are further studied, showing their consistent, symmetric, behavior throughout the tuning range.<sup>1</sup>

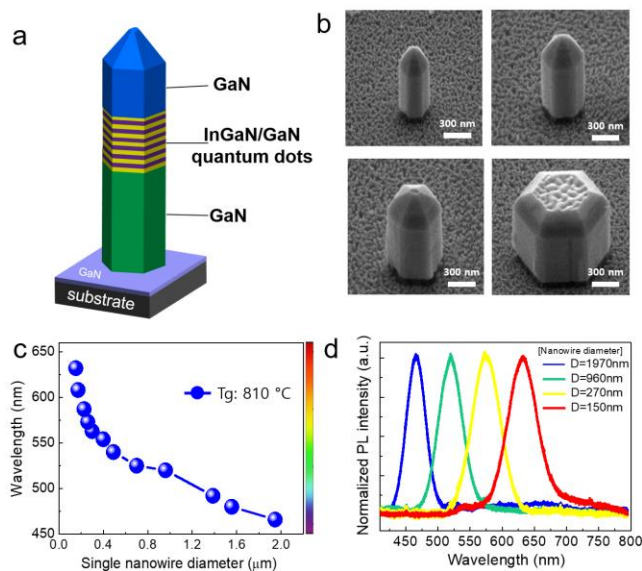


**Figure 1:**(a) Schematic of a single InGaN/GaN nanostructure. (b) SEM image of single InGaN/GaN nanowires. (c) Variations of the peak emission wavelength of single InGaN/GaN nanowires. (d) Normalized PL spectra of InGaN/GaN nanostructures in Sample II.<sup>1</sup>

Size-dependent PL emission from single MBE grown nano-structures has not been seen previously in catalyst-assisted nor spontaneously formed InGaN arrays. The mechanism is related to the diameter-dependent inclusion of In and Ga atoms during growth. Based on our recent studies,<sup>1</sup> the growth process in nanowire epitaxy consists of both directly impinging adatoms and adatoms which migrate from the vertical and lateral surfaces. Ga adatoms have much larger diffusion lengths ( $\sim 1\text{ }\mu\text{m}$ ) than In adatoms ( $\sim 100\text{ nm}$ ), especially at relatively high growth temperatures. In diffusion lengths are further limited by thermal desorption.<sup>15</sup> At high temperature, Ga diffusion length is on the same order as the diameter range of interest, and hence

the Ga adatom incorporation shows only a small dependence on structure size. In incorporation should be significantly reduced as diameter increases, since In adatom incorporation due to lateral diffusion will decrease. Directly impinging In adatoms are independent of structure diameter, since the beam equivalent pressure (BEP) is constant across the growth area. In contrast, diameter has a strong effect on In inclusion from lateral diffusion. This results in a relative decrease in In content and a corresponding bluer emission wavelength (see Figures 1c and d). The variation of emission color is thus largely dependent on each individual nano-structure's diameter, and not on any global effects. These results differ from what is observed in ensemble InGaN nanowires grown by SAG with high packing density,<sup>15,19,20</sup> which due to shadowing show a redshift in emission with increasing diameter.

### Full-color Electroluminescent LEDs

We have designed single nanowire LED groupings consisting of nanowires with varying diameters in order to demonstrate full-color (red, green, and blue – RGB) tunable single nanowire LED pixels integrated on the same chip. The LED nanostructures consist of 0.44  $\mu\text{m}$  n-GaN, six InGaN/GaN quantum discs and 0.15  $\mu\text{m}$  p-GaN.<sup>1</sup> Growth conditions can be determined such that emission wavelengths across the visible spectral range can be realized for nanowires with diameters varying from  $\sim 200\text{ nm}$  to  $\sim 600\text{ nm}$ , a much smaller range than in the previous experiments. Pattern design took into account the lateral growth effect previously discussed. The LEDs have an average height of 650 nm, with hexagonal shape and smooth side facets, which contributes to light emission from the top surface of each LED. Nano-LEDs of this design also exhibit high light extraction efficiency.

Figure 2a depicts multi-color single nanowire InGaN/GaN nano-LEDs formed on a single chip. A polyimide planarization layer was spin-coated over the as-grown nanostructures to initially cover the nanowires, which was subsequently etched to reveal the top surface of nanowires. Thin Ni (7 nm)/Au (7 nm) electrodes were then deposited on the exposed top surface of individual nanowires and annealed at  $\sim 500\text{ }^\circ\text{C}$  for 1 min in nitrogen. A 100 nm layer of indium tin oxide (ITO) was deposited to serve as a current spreading electrode. The complete LEDs were then annealed at  $300\text{ }^\circ\text{C}$  for 1 hour under vacuum. N-GaN contacts are then deposited.

Typical performance characteristics of single wire nano-LEDs are shown in Figure 2. Representative I-V curves of the blue ( $D \sim 630\text{ nm}$ ), green ( $D \sim 420\text{ nm}$ ), orange ( $D \sim 320\text{ nm}$ ) and red ( $D \sim 220\text{ nm}$ ) LEDs, are shown in Figure 2b. The turn-on voltages are similar to the semiconductor bandgap, significantly improved from previously shown ensemble LEDs and green and red GaN-based planar devices.<sup>14,21</sup> Current densities as high as  $7\text{ kA/cm}^2$  were measured at  $\sim 3\text{ V}$ , with the highest current densities possible in nano-LEDs with the smallest diameters. This corresponds to the enhanced doping levels in smaller diameter nanostructures and the resulting effect on carrier density,<sup>22,23</sup> as well as increased heat dissipation.<sup>14</sup> This suggests that nano-scale optoelectronic devices can be driven at extremely high current density and brightness compared with conventional planar devices. Leakage current measured under reverse bias is also quite small, but is a function of diameter, likely due to defects in larger structures. This is in reasonable agreement with previously published studies.<sup>24,25</sup>

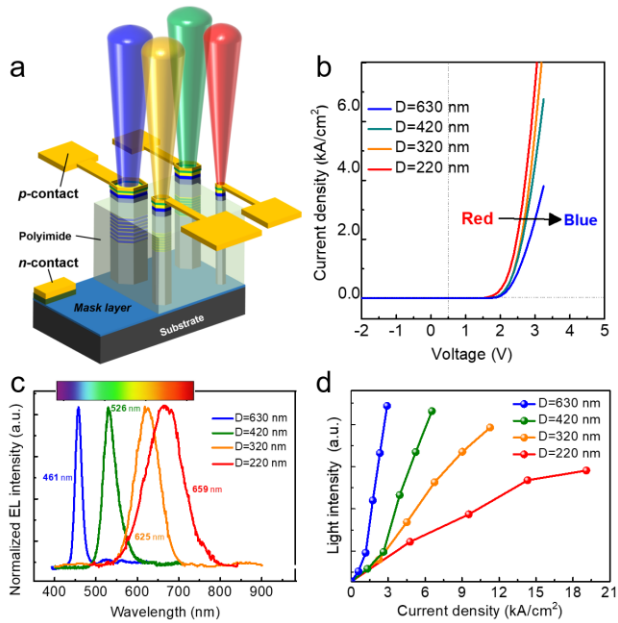


**Figure 2:** (a) Schematic illustration of monolithically integrated multi-color single nanowire LED pixels on a single chip. (b) Current-voltage characteristics of single nanowire LEDs. (c) Electro-luminescence (EL) spectra of single nanowire LEDs. (d) Light-current characteristics of single nanowire devices.<sup>1</sup>

These nano-LEDs also show novel light emission properties. Electroluminescence (EL) was collected using a fiber-coupled spectrometer. Figure 2c plots the EL spectra of individual sub-pixels with diameters of 220, 320, 420 and 630 nm, with peak emission wavelengths of 659, 625, 526 and 461 nm, respectively. The spectra are taken at currents of approximately 5  $\mu$ A. Figure 2d shows light-current (L-I) characteristics of the red, orange, green, and blue nano-LEDs. One can see that the EL intensity increases with injection current approximately linearly. Light intensity was greater in devices with larger diameters under identical current density, because of the larger effective area. Nano-LEDs with smaller areas could also be operated at higher current density, which we attribute to their more efficient conduction and thermal dissipation. The emission peak is nearly invariant with increasing current, demonstrating that the quantum-confined Stark-effect is minimal, which is in turn due to the efficient strain relaxation of such nano-structures. By controlling the nanowire diameter and height, single nanowire nano-LEDs can have significantly increased light extraction efficiency, along with a more controllable emission cone, compared to planar LEDs. We also note that these devices are capable of sustaining massive current densities, with linear increases in light output sustained into the kA/cm<sup>2</sup> regime, roughly 100x the typical operating current density of a planar LED. This implies a peak brightness well into the million nit regime.

### Photonic Bandgap Effects in LEDs

Such sub-micron devices demonstrate that even single nanostructure LEDs can be made to be efficient and controllable. However, today's displays, even the highest resolution micro-displays, rarely call for pixel sizes that are ~200nm in extent. Instead, microdisplay technology is striving

to push from 5-10 $\mu$ m pixel pitches today to 1-3 $\mu$ m in the near future. Similarly, microLED display approaches require enough light to be emitted for daylight viewing, and for mass-transfer methods to be able to handle the tiny devices. Conventional wisdom is that again, devices in the size range of 1-5 $\mu$ m are probably ideal. So while a single nano-LED is of interest, a small array of such structures is likely necessary for near-term commercial relevance.

Figure 3 shows a micrograph of such an array of nanostructures. The same degree of growth control is possible for such an array, leverage the same selective area epitaxy approaches utilized to grow the singular structures above. After the wires are grown, similar lithography steps can be employed to place a contact over the array, and this contact thereby defines the device active area.

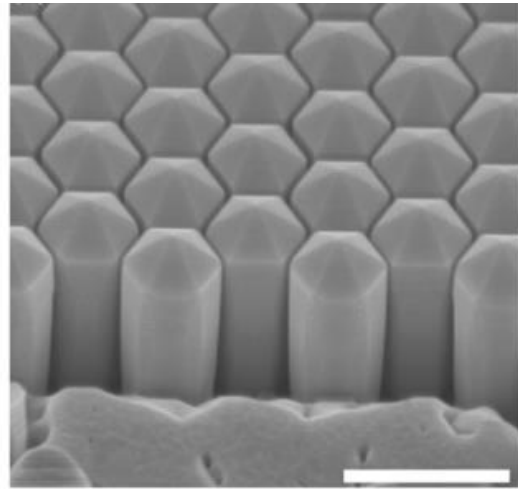


**Figure 3:** A scanning electron microscope image of a small dense array of InGaN nanostructures, such as were used in the single nanowire LEDs above. The scale bar represents 500nm.

Arrays of such structures are useful for more than just scaling up the area, brightness, and handling ease of such LEDs. Through careful design of the diameters, spacing, and periodicity of the nanostructures, the periodic fluctuations of index of refraction can simultaneously create a photonic bandgap effect. Such effects have been previously shown in photoluminescence<sup>26</sup>, but never in an operating electroluminescent, non-lasing, device.

Such photonic bandgap LEDs (PBG-LEDs) have been fabricated, and exhibit the combined benefits of nanoLEDs such as are in this paper (efficient emission, superior crystallinity with high indium doping, controlled growth of RGB emitters on a single substrate), with photonic crystal effects. These PBG-LEDs exhibit ultra-narrow-band emission, and have a peak emission wavelength that is independent of temperature and current. PBG-LEDs could indeed be the most credible pathway to true 100% Rec.2020 color gamut, without resorting to laser sources with their inherent challenges relating to speckle. In enhancing the emission for a single color of light, the photonic bandgap effect also speeds the emission of light, increasing efficiency<sup>26</sup>. Finally, this enhanced wavelength of emission also corresponds to an enhanced direction of emission, and so these PBG-LEDs are also extremely narrowband directional emitters.

To demonstrate this directional feature of the devices, the far-field angular distribution of the emission was studied by



collecting EL emission with a fiber mounted on a rotation stage. The distance between the fiber and the PBG-LED is one inch. The EL intensity at each emission/collection angle was calculated by integrating over the emission's spectral range. Shown in Fig. 4 is the angular distribution of the EL intensity. It is seen that the emission is mainly distributed along the vertical direction, with a divergence angle  $\sim 10$  degrees. Such optics-free, highly directional emission is directly related to the surface-emission mode of the InGaN photonic nanocrystal structures shown earlier. This property can greatly simplify the design and reduce the cost of next-generation ultrahigh resolution display devices and systems, especially where etendue of the optical system is limited.

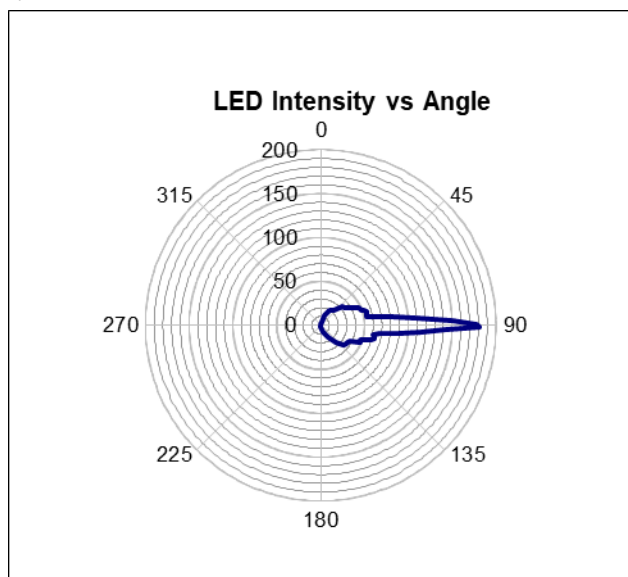


**Figure 4:** Far-field angular distribution of electroluminescence intensity.

#### 4. Impact

We have shown multi-color, single nanowire LEDs on a single chip, grown in a single process step, by using selective growth. Compared to conventional devices, such nano-LEDs offer several technological advantages, including significantly enhanced light extraction efficiency, controllable radiation cones, tunable visible light emission, and efficient current conduction. Due to their nano-size and reduced capacitance, such devices also offer ultrahigh speed frequency response. This provides a unique platform for realizing tunable, full-color nanoscale LEDs for a range of markets, including high resolution imaging and displays, lighting, communications, sensing, and medical diagnostics. The implications for microLED displays are clear and large, offering high efficiency LEDs that can be as small as 100nm, with the full visible spectrum accessible in a single materials system and grown on a single wafer in a single process step. Combined with the possible photonic bandgap effects available in small arrays of such structures, the potential applications of this technology are limitless.

#### 5. References

1. Ra, Y.H. et al. *Nano Lett.* 2016, 16, 4608-4615.
2. Krames, M. R.; Shchekin, O. B.; Mueller-Mach, R.; Mueller, G. O.; Zhou, L.; Harbers, G.; Craford, M. G. *J. Display Technol.* 2007, 3, 160-175.

3. Nakamura, S.; Senoh, M.; Iwasa, N.; Nagahama, S. *Appl. Phys. Lett.* 1995, 67, 1868-1870.
4. Shen, C.; Ng, T. K.; Ooi, B. S. *Opt. Express* 2015, 23, 7991-8
5. Sousa, M. A.; Esteves, T. C.; Sedrine, N. B.; Rodrigues, J.; Lourenco, M. B.; Redondo-Cubero, A.; Alves, E.; O'Donnell, K. P.; Bockowski, M.; Wetzel, C.; Correia, M. R.; Lorenz, K.; Monteiro, T. *Sci. Rep.* 2015, 5, 9703.
6. Kishino, K.; Ishizawa, S. *Nanotechnology* 2015, 26, 225602.
7. Wang, R.; Nguyen, H. P.; Connie, A. T.; Lee, J.; Shih, I.; Mi, Z. *Opt. Express* 2014, 22 Suppl 7, A1768-75.
8. Wang, R.; Ra, Y.-H.; Wu, Y.; Zhao, S.; Nguyen, H. P. T.; Shih, I.; Mi, Z. *Proc. SPIE* 9748 2016, 9748, 97481S.
9. Gago-Calderón, A.; Fernández-Ramos, J.; Gago-Bohórquez, A. *Displays* 2013, 34, 359-370.
10. Chen, E.; Guo, T. *Displays* 2014, 35, 84-89.
11. Choi, M. K.; Yang, J.; Kang, K.; Kim, D. C.; Choi, C.; Park, C.; Kim, S. J.; Chae, S. I.; Kim, T. H.; Kim, J. H.; Hyeon, T.; Kim, D. H. *Nat. Commun.* 2015, 6, 7149.
12. Kim, S.; Kwon, H. J.; Lee, S.; Shim, H.; Chun, Y.; Choi, W.; Kwack, J.; Han, D.; Song, M.; Kim, S.; Mohammadi, S.; Kee, I.; Lee, S. Y. *Adv. Mater.* 2011, 23, 3511-3516.
13. Yanagihara, A.; Ishizawa, S.; Kishino, K. *Appl. Phys. Lett.* 2014, 7, 112102.
14. Gong, Z.; Jin, S.; Chen, Y.; McKendry, J.; Massoubre, D.; Watson, I. M.; Gu, E.; Dawson, M. D. *J. Appl. Phys.* 2010, 107, 013103.
15. Sekiguchi, H.; Kishino, K.; Kikuchi, A. *Appl. Phys. Lett.* 2010, 96, 231104.
16. Kishino, K.; Sekiguchi, H.; Kikuchi, A. *J. Cryst. Growth* 2009, 311, 2063-2068.
17. Bengoechea-Encabo, A.; Barbagini, F.; Fernandez-Garrido, S.; Grandal, J.; Ristic, J.; Sanchez-Garcia, M. A.; Calleja, E.; Jahn, U.; Luna, E.; Trampert, A. *J. Cryst. Growth* 2011, 325, 89-92.
18. Urban, A.; Malindretos, J.; Klein-Wiele, J. H.; Simon, P.; Rizzi, A. *New J. Phys.* 2013, 15, 053045.
19. Kishino, K.; Yanagihara, A.; Ikeda, K.; Yamano, K. *Electron. Lett.* 2015, 51, 852-854.
20. Kishino, K.; Nagashima, K.; Yamano, K. *Appl. Phys. Express* 2013, 6, 012101.
21. Wang, R.; Liu, X.; Shih, I.; Mi, Z. *Appl. Phys. Lett.* 2015, 106, 261104.
22. Kibria, M. G.; Zhao, S.; Chowdhury, F. A.; Wang, Q.; Nguyen, H. P.; Trudeau, M. L.; Guo, H.; Mi, Z. *Nat. Commun.* 2014, 5, 3825.
23. Zhao, S.; Connie, A. T.; Dastjerdi, M. H.; Kong, X. H.; Wang, Q.; Djavid, M.; Sadaf, S.; Liu, X. D.; Shih, I.; Guo, H.; Mi, Z. *Sci. Rep.* 2015, 5, 8332.
24. Wei, T.; Huo, Z.; Zhang, Y.; Zheng, H.; Chen, Y.; Yang, J.; Hu, Q.; Duan, R.; Wang, J.; Zeng, Y.; Li, J. *Opt. Express* 2014, 22 Suppl 4, A1093-100.
25. Shan, Q.; Meynard, D. S.; Dai, Q.; Cho, J.; Schubert, E. F.; Kon Son, J.; Sone, C. *Appl. Phys. Lett.* 2011, 99, 253506.
26. Ra, Y.H. et al. *Adv. Funct. Mater.* 2017, 1702364.

